



PAM: Discrete 3-D Model of Tumor Dynamics in the Presence of Anti-tumor Treatment

Marta Panuszewska^(✉), Bartosz Minch, Rafał Wcisło, and Witold Dzwiniel

Department of Computer Science, AGH University of Science and Technology,
Krakow, Poland
panuszewska@agh.edu.pl

Abstract. Existing computer models of cancer focus mostly on disease progression rather than its remission/recurrence caused by anti-cancer therapy. Herein, we present a discrete model of tumor evolution in 3D, based on the Particle Automata Model (PAM) that allows for following the spatio-temporal dynamics of a small neoplasm (millimeters in diameter) under treatment. We confront the 3D model with its simplified 0D version. We demonstrate that the spatial factors such as the vascularization density, absent in the structureless 0D cancer models, can critically influence the results of treatment. We discuss briefly the role of computer simulations in personalized anti-cancer therapy.

Keywords: Tumor dynamics
3-D particle automata computer model
Anti-tumor treatment simulation

1 Introduction

Even though the mortality rate of cancer is slowly decreasing, it is still one of the main fatality factors worldwide. Approximately 40 percent of people will be diagnosed with some type of cancer at one point during their lifetime [1]. Development of an effective general anti-cancer treatment strategy is vastly restricted because the neoplasms greatly differ between each other. Moreover, the microenvironment of tumor evolution defined by bio-mechanical properties of a tissue and its vascularization can be completely different not only for various cancer types but also for various patients and even parts of attacked tissue. Computer model of a tumor that mimics its evolution before and after treatment for a specific patient, can help in control of principal tumor progression/recession mechanisms and in predicting possible scenarios of its dynamics, thus in development of optimal personalized anti-cancer therapy.

Tumor growth, regression/recession and recurrence are complex, multi-scale phenomena, influenced by countless mutually coupled microscopic and macroscopic factors (see e.g. [24]). The taxonomy of cancer models includes broad spectrum of homogeneous (discrete, stochastic, continuous: single-phase and multi-phase) and heterogeneous (discrete-continuous) computational paradigms. They

are employed for modeling both very detailed processes of oncogenesis occurring in a single spatio-temporal scale (in molecular, tissue or organism level) and complex multiscale systems. Diversity of existing tumor models are described in comprehensive books from computational oncology (e.g. [6, 18, 24]) and hundreds of papers.

Cancer dynamics can be simulated by means of both very simple 0D models described by ODEs (ordinary differential equations) and more complicated, computationally demanding spatio-temporal 3D systems (realized numerically by using finite element methods FEM, agent-based discrete models etc.) [21, 23, 24]. The latter ones are focused mostly on tumor progression. Meanwhile, its remission/recurrence caused by anti-cancer therapy is rather modeled by using simpler ODEs based codes [20, 25]. This is understandable because the 3D tumor models are usually over-parametrized. Taking into account the processes responsible for the anti-cancer therapy may result in additional excessive increase of their complexity. Consequently, this can considerably lower the quality of predictions of cancer dynamics due to overfitting, ill-conditioning and high computational complexity of the models.

Therefore, simple 0D computer models of cancer, adapted to real data representing tumor dynamics [21], which exploits prediction/correction scheme (such as in [7]), could seem to be more useful in predictive diagnosis systems. On the other hand, because the variability of their parameters is prohibitively high and depends strongly on the microenvironment of cancer dynamics, the elaborated prognoses are too often inconclusive [21]. That is why, employing advanced image diagnostics of the future as input data, 3D models could be extremely helpful both in recognizing the most critical regression and recurrence factors and in the process of detailed analysis of various scenarios of tumor evolution. Especially, in respect to the specific tumor environment such as bio-mechanical properties of tissue and its vascularization topology. We expect that balanced use of tumor models of various complexity together with the new opportunities of the computational and diagnostic technologies will decide about usefulness of predictive oncology in personalized anti-cancer therapy in the future.

The main contribution of this paper is the application of 3D PAM modeling paradigm [8] in simulating cancer dynamics, assuming treatment. The 3D model considers the most important factors influencing cancer remission caused by the anti-tumor therapy. The PAM model allows for simulating the tumor evolution in the mesoscopic scale (a millimeter in diameter, i.e., $N = 10^5 - 10^6$ cells) in a reasonable CPU time on a laptop computer. Simulation time for a greater systems, scales up linearly with N . We also developed the method for generating realistic vascular network structure, which can be easily adapted to various tissues. Additionally, by assuming different types of interactions between cells, the extended PAM model reflects more realistic bio-mechanical properties of cancerous tissue in which the rheological properties of “healthy” and tumor cells are distinctly different. We aim to demonstrate that our model constitutes an important complement to approximate 0D tumor models, which are currently of clinical use [3, 19, 21]. Our goal is to show that the 3D model is sensitive to a spe-

cific tumor micro-environment defined by the density of tissue vascularization, which is a crucial factor determining the result of anti-cancer therapy.

In the following section we present a simple structureless 0D model of tumor dynamics, which was applied in clinical practice and is a good approximation of our 3D solution. Next, we briefly describe the 3D PAM model of cancer evolution under treatment and the computational layout, which mimics realistic tissue vascularization. We describe some computer experiments showing the influence of the tissue vascularization density on the tumor evolution under treatment. Finally, we discuss the conclusions.

2 Simplified 0D Cancer Model

The 0D tumor model [21] is presented schematically in Fig. 1. It is assumed that there are three basic types of tumor cells: proliferative P , quiescent Q and mutated quiescent Q_P . We assume also that only the proliferative cells are able to reproduce. The proliferative tumor cells, which stay some time in a very hostile environment (e.g. low concentration of oxygen and nutrients, high pressure etc.) become quiescent. In case of anti-tumor treatment, the proliferative cells die and the damaged (mutated) quiescent cells appear, which can either die, stay dormant or revert (after some time) to proliferative state, becoming “the seeds” of even more voracious cancer. The model is defined by the set of four ODEs. Each of them describes the dynamics of the population of a specific cell type. The equations are as follows [21]:

$$\frac{dC}{dt} = -T_C C, \quad (1) \qquad \frac{dQ}{dt} = k_{PQ} P - \gamma_Q C T_C Q, \quad (2)$$

$$\frac{dQ_P}{dt} = \gamma_Q C T_C Q - k_{QP} Q_P - \delta_{QP} Q_P, \quad (3) \qquad P^* = P + Q + Q_P, \quad (4)$$

$$\frac{dP}{dt} = \lambda_P P \left(1 - \frac{P^*}{K}\right) + k_{QP} Q_P - k_{PQ} P - \gamma_P C T_C P. \quad (5)$$

where: P - the total volume of proliferative cells; Q - the total volume of quiescent cells; Q_P - the total volume of mutated quiescent cells; C - anti-cancer drug concentration; T_C - a constant used for calculating decrease of anti-cancer drug concentration; λ_P - a rate of growth for P ; k_{PQ} - a rate the cells change their states from P to Q ; k_{QP} - a rate the cells change their states from Q_P to P ; γ_Q, γ_P - damage rates in proliferative and quiescent tissue, respectively.

In [21], the model parameters were adapted to real data - glioma cancer evolution - which were taken from many (more than 300) patients for three types of anti-cancer therapies. In Fig. 2 we can see two examples of tumor size dynamics for two different (averaged) “patients”, obtained by solving the model equations. Herein, we have chosen the averaged set of model parameters obtained for PCV chemotherapy and trained additionally by using Bayesian adaptation technique (ABC) [5]. Despite apparent differences, we can remark that the tumor evolution

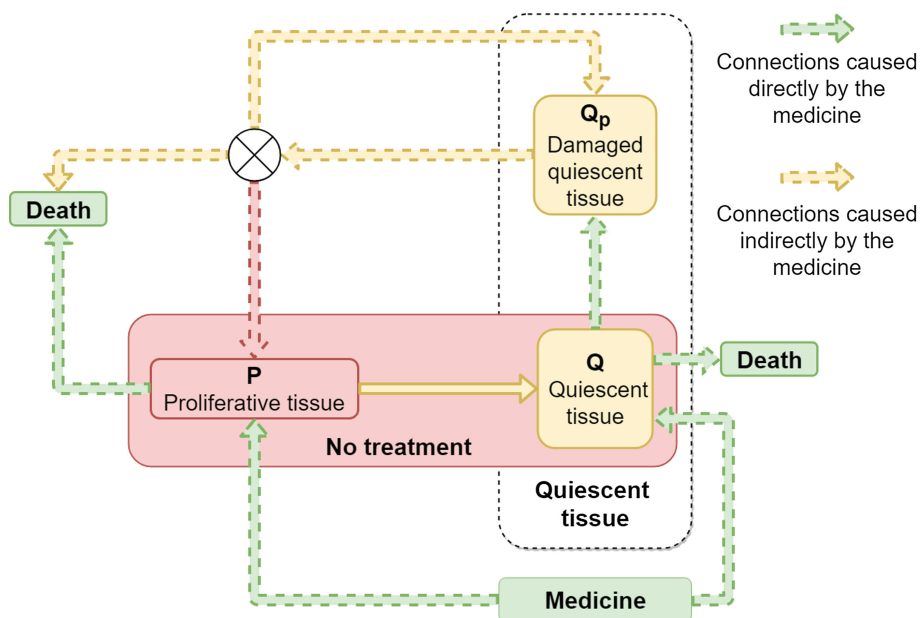


Fig. 1. Block diagram of the 0-D cancer model.

is very similar in both cases. The tumor increases in size at the beginning of the simulation, then rapidly shrinks due to treatment and, finally, some time after treatment it re-grows again. This simple model applies to rather big tumors, i.e., up to 8 cm of mean tumor diameter (MTD) [21]. Our 3-D model is able to simulate tumor of much more modest size - up to a millimeter in diameter (on a laptop computer). Thus, we expect the tumor evolution type such as that for the “first patient” with early tumor symptoms (see Fig. 2). As shown in [21], for the majority of cases, typical not optimistic result is observed - an inevitable and very quick re-growth of tumor mass. We demonstrate in Fig. 2 that a wrong choice of treatment plan, or its abrupt discontinuation, can result in a rapid tumor recurrence. For example, as shown in Fig. 2, the tumors of the two “patients” may be similar in size after 50 months of their appearance, despite the patients started their therapies in very different stages of tumor development. In the ideal case presented in Fig. 2, i.e., when the size of real tumor evolution follows exactly the model (1–5), we are able to predict tumor size dynamics not only after but also before treatment. The predictions were made by training the model (i.e., adapt its parameters from data) by using the Bayesian adaptation technique (ABC) [5] employing continually “measured” tumor volume in a relatively short time interval Fig. 2. On the other hand, as shown in [21], due to rather scarce and not accurate data, and most of all, incompatibility between the 0-D model and the reality, the quality of model predictions is definitely worse. Therefore, even though the 0D model can be very useful, it cannot extrapolate long term changes

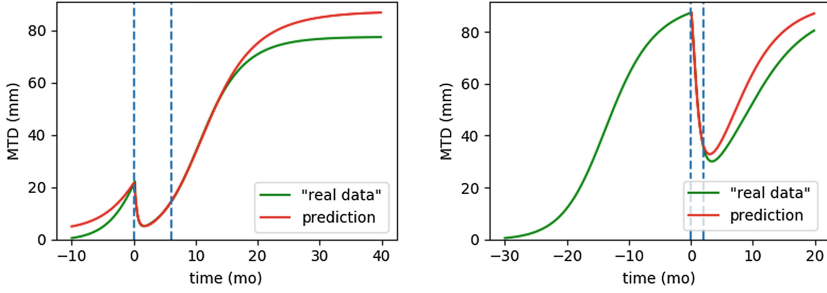


Fig. 2. Tumor volume in time, for two “patients”. The green line represents the exact solution of the equations (1–5). The red line delineate the predictions based on data located between blue dashed lines. (Color figure online)

in the tumor spatial dynamics stimulated by the non-homogeneous density of tissue and vascularization, e.g., caused by occurrence of voids due to necrosis and vascular remodeling processes, respectively. Thus, the model parameters should be continuously corrected in the course of treatment. The 3D tumor model could help in better adjustment of the approximate 0D model to real data. Assuming that in the future we will be able not only to measure the tumor size in real time but also to observe its shape and biological structure of its growth environment, we can think about application of more sophisticated 3-D tumor models in predictive oncology. Knowing the real initial tumor layout, we would be able to predict spatial scenarios of its evolution taking into account that a specific tissue structure (its mechanical properties and/or density of vasculature) could block or accelerate its dynamics. Particularly, it might be possible to see if the cancer does not start to re-grow in a location where the access to the anti-cancer drug is restricted (for example, in a small tissue fragment which is away from blood vessels). This information plays a key role in choosing a therapy plan and decide about the way of its application, e.g., the dose and frequency of drug administration.

3 3D Tumor Model

3.1 Particle Automata Model

We extended the 0D model of tumor with treatment to three dimensions. To this end we adapted the PAM heterogeneous discrete-continuous modeling paradigm [8, 23] to the framework from Fig. 1. The basic properties of 3D PAM model are described below.

As shown in Fig. 3a, the system consisting of tumor and healthy tissue can be represented by interacting cells (particles) with a few variable states. The particle system is bounded by a computational box under a constant external pressure. Each particle i (cell) is defined as a tuple $(\mathbf{x}_i, \mathbf{v}_i, \mathbf{a}_i)$, where: i - particle index and $(i = 1, \dots, N)$, \mathbf{r}_i - its position, \mathbf{v}_i - velocity, \mathbf{a}_i - attributes (states).

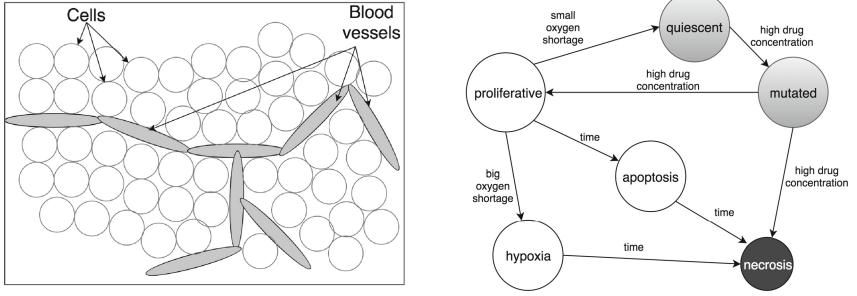


Fig. 3. The scheme of main components of the Particle Automata Model and cell states. (a) Particles representing tissue cells and blood vessels. (b) Life cycle of a cell. We mark in gray the states possible only for tumor cells.

Each particle represents a tissue cell while two particles create a single segment of a blood vessel. The blood vessels are made of connected segments. The vector of particle attributes \mathbf{a}_i includes information on: the cell type (tumor: {proliferative, quiescent, mutated}, healthy, blood vessel}, a phase of the cell life-cycle (see Fig. 3b), cell size, cell age, hypoxia time, concentrations of O_2 , TAF (tumor angiogenic factor) and anti-tumor drug, and total pressure exerted on a particle from the rest of the tissue. The spring-like forces [8] between particles mimic mechanical repulsion and attraction between cells. The total force acting on a particle i is the sum of all forces from other surrounding particles in a given cut-off radius. The particles of all types move according to the ODE system of the Newtonian equations of motion, while their states follow automata rules (defining, e.g., cell life-cycle from Fig. 3b, thresholding rules, chemical interactions between neighboring cells etc.). The blood pressure in the vessels is approximated by the Kirchhoff law. Spatio-temporal evolution of each cell is highly dependent on the concentrations of oxygen (and TAF in angiogenic phase) and anti-tumor drugs calculated in a cell position by solving continuous reaction-diffusion PDEs. The concentrations define internal state of each cell. The blood vessel network Ω releases in each time step a constant amount of oxygen and anti-tumor drugs (sources), which diffuse inside the tumor mass. Simultaneously, the diffusive oxygen and drugs are consumed in a given constant rate by the tissue cells (sinks).

3.2 The Layout and Blood Vessel Network

We have developed a simple algorithm that allows us to generate a realistic, non-deterministic vessel network being the approximation of more sophisticated approaches presented in [17, 22]. We assumed that all the vessels consist of a series of line segments of the length equal to “*vessel.length*”. Starting and ending points of the vessels are chosen at the left and right sides of bounding box. Their radii are defined by “*max.thickness*” parameter. Then, the subsequent layers of vessel segments are added towards the center of the computational box with

randomly chosen curvature from 0 to “*max_curvature*” interval. Each vessel segment has a chance to split into two vessels with a probability “*chance_of_split*”. The thickness of a blood vessel segment is inversely proportional to its distance to the center of the computational box. The number of layers of vessel segments is defined by “*levels*” parameter. When all the layers are created, we connect each blood vessel to the nearest neighbor. In Fig. 4, we present the layouts we used in our experiments.

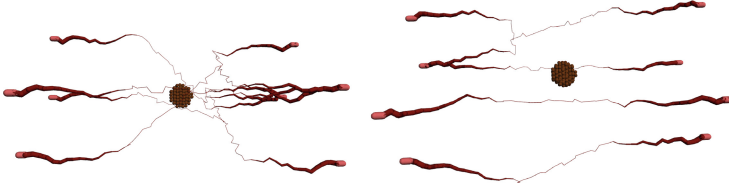


Fig. 4. The layouts of the tissue model with dense (left) and poor vasculature (right). Healthy cells are hidden for visualization purposes.

Finally, the tissue cells surrounding the vessels are added. All of the cells are arranged in densely packed layers. The initial cluster of tumor cells is situated at the center of the computational box.

3.3 Viscosity of the Tissue

In the PAM model we have introduced a new model of interparticle forces. The healthy and cancerous tissues are represented by viscous SPH particles. Then, the whole particle ensemble simulates the dynamics of a multiphase Navier-Stokes fluid. The main reason for this assumption is the possibility to mimic real differences between rheological properties of tumor and healthy tissues (the healthy cells are more “viscous”). For smaller tumors, this difference in viscosity makes tumor cells much more flexible what is demonstrated in Fig. 5.

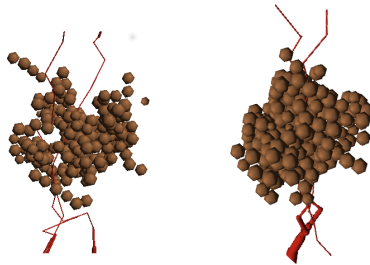


Fig. 5. Comparison of PAM simulations with and without SPH properties of viscosity force. Left: with viscosity force. Right: without viscosity force.

For larger tumors this difference in viscosity does not reveal in observed growth patterns. The pressure exerted on the tumor and its fluctuations are too small to trigger tumor surface instability effects. Therefore, the avascular tumors can evenly grow in all directions. We anticipate that, the surface instabilities can be visible for larger tumors (over 1 cm in diameter), for which the fingering instability can be expected, as it is in large ensembles of DPD (dissipative) particles in [9].

3.4 Anti-cancer Treatment

The PAM model of the tumor behavior after treatment is based on the same assumptions as the 0-D model [21]. We assume that all the tumor cells start their life cycle as the proliferative ones. If the oxygen concentration drops below a given threshold the proliferative cells become quiescent, i.e., they will no longer have the capability to replicate. If the medicine concentration is above a certain level, the proliferative cells die and the mutated quiescent cells appear [4]. If the medicine concentration will stay high, the mutated quiescent cells will either stay mutated (but dormant), die or become proliferative once again [14, 18] being the sources of cancer re-growth. The tumor transforms from homogeneous to heterogeneous one.

Changes in drug concentration are governed by the mechanisms of medicine impact, transport&redistribution (diffusion and advection) and elimination (decay and cellular uptake), similar as in [15]. We assume, that drugs are secreted by the functional and permeable (destroyed by vascular remodeling process) blood vessels at a constant rate. The cells also consume the medicine at a constant rate, depending on a tissue type. The medicine diffusion is governed by the diffusion-reaction equation:

$$\frac{\partial C}{\partial t} = D_c \cdot \Delta C - N_r C - T_c C + c \cdot h(\Omega, T - t), \quad (1)$$

where: N_r - drug consumption rate, D_c - medicine diffusion constant, C - drug concentration, T_c - a constant used for calculating decrease of anti-cancer drug concentration, c - medicine source rate in the blood network Ω during time T . For the sake of simplicity, constant drug secretion c and its absorption $T_c C$ rates by the tissue are assumed. The function $h(x, t) = 1$, for $t > 0$ and $h(x, t) = 0$, for $t < 0$. Our assumptions are consistent with the simple model described in Sect. 2 [21]. Comparing to the fully continuous drug diffusion model [15], the advection of drug in PAM is realized by moving particles. Therefore, the advection term $v \cdot \nabla C$ is lacking in (6).

4 Results of Simulation

The size of a fragment of tissue modeled was limited to $3.0 \cdot 10^5$ cells in total. This bound is defined mostly by the computational power we dispose for simulations. They have been run on a single core of the CPU specified in Table 1. One

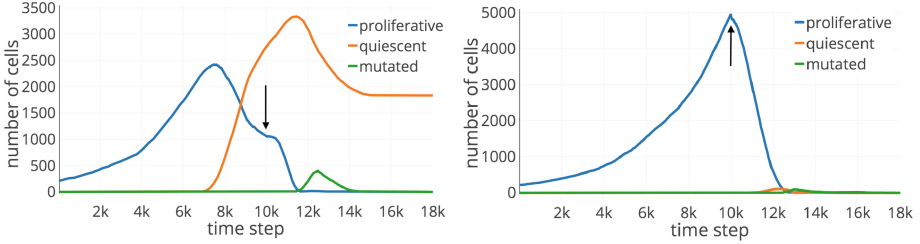


Fig. 6. Tumor evolution for the setups with (a) poor and (b) dense vasculature. The treatment was administered on the step marked with a black arrow.

simulation needs around 24 h CPU time for simulating $1.6 \cdot 10^4$ time steps. The initial setup of the simulations (Fig. 4) assumes around 200 cancer cells placed in the middle of the layout. In Table 2 we collected the most important parameters influencing tumor dynamics.

Table 1. Specification of the machine running the simulations.

CPU	Intel®Core™i7-5960X @ 4.2 GHz (8 cores, 16 threads, 20 MB of L3 cache)
RAM	DDR4 2666 MHz 32 GB (4 × 8 GB Quad-Channel)
Disk	Samsung NVMe SSD 960 Pro
GPU	nVidia GeForce GTX 1080

As shown in the previous section, the tumor evolves in a fragment of tissue composed of healthy cells and blood vessels. The proliferative and quiescent cells, being the components of the cancerous tissue, have different properties than the healthy cells and the vessels. The latter are more resistant to pressure and low oxygen concentration. The proliferative cells consume more oxygen and are very susceptible to anti-cancer drugs. These properties allow them, on the one hand, for rapid reproduction under favorable conditions and, on the other, fast necrosis (death) due to devastating effects of treatment. The quiescent cells are more resistant on the anti-cancer drugs and need extremely little oxygen to stay alive.

To show how the spatial topology of tissue exploits these cell properties and influences cancer evolution during and after treatment, we have compared tumor dynamics for two different layouts (see Fig. 4). In the first one, the tumor is well oxygenated by a dense vasculature, while in the other it is situated in a poorly vascularized tissue. As we can see in Fig. 6, after growth phase, the tumors collapse due to treatment (see also Figs. 7 and 8).

However, the results from Figs. 6 and 7 show that eradication of the tumor in the layout with poorer vasculature can fail. The tumor shrinks down during

Table 2. The most important parameters of the simulation (concerning tumor growth).

Name	Description	Value	Units
force_r_cut	Cut-off radius in forces calculations	10	μm
p_o2	O2 threshold to change state proliferative cells	0.7	norm.
q_o2	O2 threshold to change state for quiescent cells	0.35	norm.
diff_O2	Diffusion coefficient for O2	2000	p.u.
diff_med	Diffusion coefficient for medicine	4000	p.u.
time_apop	Time to apoptosis	3600	p.u.
min_inter_time	Minimum interphase time	600	p.u.
max_pressure_h	Max pressure in healthy cells	$1 * 10^{-16}$	p.u.
max_pressure_t	Max pressure in tumor cells	$1 * 10^{-15}$	p.u.
cons_rate_h	Medicine consumption rate in healthy cells	$2 * 10^{-12}$	$p.u.h^{-1}$
cons_rate_t	Medicine consumption rate in tumor cells	$2 * 10^{-11}$	p.u.
o2_cons_h	O2 consumption rate in healthy cells	$5 * 10^{-11}$	p.u.
o2_cons_t	O2 consumption rate in proliferative cells	$1 * 10^{-10}$	p.u.
o2_cons_q	O2 consumption rate in quiescent cells	$2 * 10^{-11}$	p.u.
o2_hypoxia	O2 threshold for entering hypoxia state	0.01	p.u.

*p.u. - program units, norm. - normalized

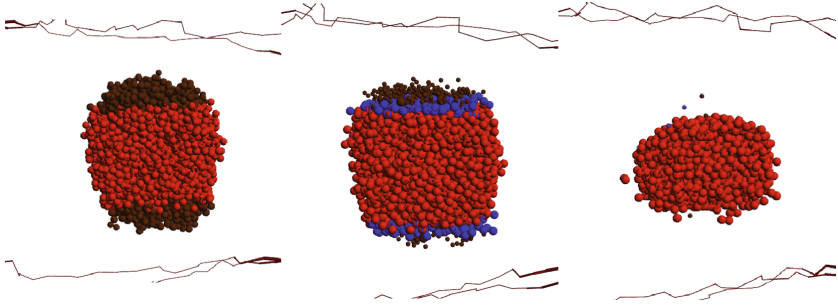


Fig. 7. Remission of the tumor in poor vasculature. The cross-section of the tumor is shown. Brown - proliferative cells, red - quiescent cells and blue - mutated. (Color figure online)

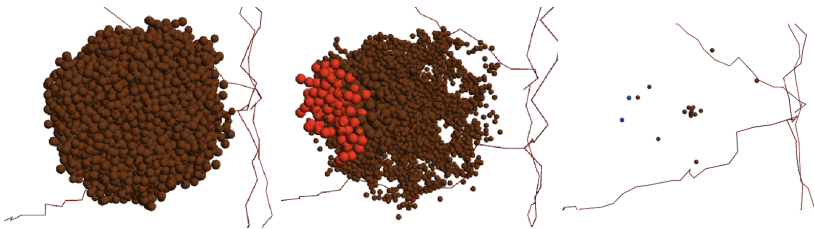


Fig. 8. Remission of the tumor in the tissue with dense vasculature.

treatment, but it can start to re-grow when the quiescent cells from tumor remnants become mutated and will convert into tumor cells. On the other hand, one can observe a dramatic decline in the number of proliferative tumor cells during treatment for the second layout. As shown in Fig. 8, for denser vasculature, due to good oxygenation, also the number of quiescent cells can be marginal. Consequently, as shown in Fig. 8 almost all cancer cell can be exterminated during treatment. These results demonstrate that the choice of the right concentration of anti-tumor drugs and the type of treatment is highly dependent on the tumor vasculature what is in full agreement with observations (see, e.g., [11]). It also shows that anti-angiogenic therapy - which inhibits tumor vascularization - in the incipient stages of tumor grow may be very risky [11]. One can expect that if anti-angiogenic therapy fails, more demanding chemotherapy need to be applied, what leads to worse side effects and poor prognoses. If we compare the tumor dynamics from Fig. 6 to the tumor evolution simulated by 0-D model from Fig. 2, we can see that the results are fairly consistent. The initial growth stage and rapid decline during treatment look similar to the tumor model with a dense vasculature. The tumor regrowth is not observed due to insufficient number of quiescent cells and the death of all proliferative ones. In the second case of poor vascularization, many quiescent cells survive the treatment. Some of them, which become mutated, can be the source of further cancer recurrence. This is particularly dangerous in case of cancers with scattered consolidation (e.g. in lung cancer), i.e., evolving in the form of the cluster consisting of large number of tiny tumors. After not sufficiently destructive chemotherapy, though the most of small tumors will die, the cancer recurrence can be still feasible starting from tumor blobs such as in Figs. 6a and 7.

5 Concluding Remarks

In this paper we present the 3-D model of a small (mesoscopic) tumor simulating various phases of its evolution, particularly, remission/recurrence stimulated by anti-cancer therapy. We demonstrate that our extended PAM model reveals a strong dependence of the cancer dynamics under treatment on its spatial environment, such as the tumor vascularization. The size of simulated tumor is constrained by the high computational complexity of the PAM model and the processing power of available computer systems. However, the modeling of anti-cancer treatment even in case of the tumors of millimeters size is also very rational. Some types of cancer (e.g., lung and breast cancers) consist of many scattered clusters of tumor cells. Moreover, the increasing effectiveness of diagnostics enables us to discover minuscule tumors in very early stages of their development. Consequently, due to different size and structure of small tumors than large ones, what reveals in smaller population of mutated quiescent cells, one can expect different scenarios of tumor re-growth which require other therapy plans than those applied for larger tumors.

Although, we did not try to match the parameters of PAM model to the 0-D model (in fact, the two models presented here represent completely different

tumors) one can see that in the context of both their spatial scales and types, they behave very similarly for small tumor sizes. Thus, we believe that the calibration of the two is possible. So, afterwards, the 3-D model of tumor could be used as a “ground truth” for learning the parameters and normalization of approximated 0-D cancer model and to mimic a broad range of tumor evolution scenarios depending on its spatial structure and the environment.

Summarizing, nowadays, the 3-D model of tumor can be used as an extension and support for simpler 0-D models in personalized anti-cancer therapy. Its main disadvantage is the large number of parameters, what can make it useless (over-fitting) when adapted to small and poor (e.g., only tumor MTD measurements) real data sets. However, in the future, having in mind, on the one hand, the fast development of medical imaging tools which soon will provide us with the realistic 3-D images of the environment of cancer evolution, and, on the other, the expected radical increase of computational power, the 3-D tumor models can soon become independent and precise tools in predictive oncology.

Acknowledgments. The work has been supported by the Polish National Science Center (NCN), in the scope of two projects: 2013/10/M/ST6/00531 (RW and BM) and 2016/21/B /ST6/01539 (MP and WD). We thank Piotr Pedrycz, (MSc student), for providing us with the results of parameters adaptation for 0-D tumor model.

References

1. American Cancer Society: Lifetime Risk of Developing or Dying From Cancer (2018). <https://www.cancer.org/cancer/cancer-basics/lifetime-probability-of-developing-or-dying-from-cancer.html>
2. Bender, J., Koschier, D.: Divergence-free smoothed particle hydrodynamics. In: Proceedings of ACM SIGGRAPH/EUROGRAPHICS Symposium on Computer Animation (SCA) (2015)
3. Benzekry, S., Lamont, C., Beheshti, A., Tracz, A., Ebos, J.M.L., Hlatky, L.: Classical mathematical models for description and prediction of experimental tumor growth. *PLoS Comput. Biol.* **10**(8), e1003800 (2014)
4. Chabner, B.A., Longo, D.L.: Cancer Chemotherapy and Biotherapy: Principles and Practice. Lippincott Williams and Wilkins, Philadelphia (2011)
5. Csilléry, K., Blum, M.G., Gaggiotti, O.E., François, O.: Approximate Bayesian computation (ABC) in practice. *Trends Ecol. Evol.* **25**(7), 410–418 (2010)
6. Cristini, V., Lowengrub, J.: Multiscale Modeling of Cancer: An Integrated Experimental and Mathematical Modeling Approach, p. 278. Cambridge University Press, Cambridge (2010)
7. Dzwinel, W., Khusek, A., Wcisło, R., Panuszewska, M., Topa, P.: Continuous and discrete models of melanoma progression simulated in multi-GPU environment. In: Wyrzykowski, R., Dongarra, J., Deelman, E., Karczewski, K. (eds.) PPAM 2017. LNCS, vol. 10777, pp. 505–518. Springer, Cham (2018). https://doi.org/10.1007/978-3-319-78024-5_44
8. Dzwinel, W., Wcisło, R., Yuen, D.A., Miller, S.: PAM: particle automata in modeling of multi-scale biological systems. *ACM Trans. Model. Comput. Simul.* **26**(3), 1–21 (2016). Article no. 20

9. Dzwinel, W., Yuen, D.A.: Rayleigh-Taylor instability in the mesoscale modeled by dissipative particle dynamics. *Int. J. Mod. Phys. C* **12**(1), 91–118 (2001)
10. Gerlee, P., Anderson, A.R.A.: Diffusion-limited tumour growth: simulations and analysis. *Math. Biosci. Eng.* **7**(2), 385–400 (2010)
11. Huang, D., et al.: Anti-angiogenesis or pro-angiogenesis for cancer treatment: focus on drug distribution. *Int. J. Clin. Exp. Med.* **8**(6), 8369 (2015)
12. Iwasa, Y., Michor, F.: Evolutionary dynamics of intratumor heterogeneity. *PLoS ONE* **6**(3), e17866 (2011)
13. Jagiella, N., Rickert, D., Theis, F.J., Hasenauer, J.: Parallelization and high-performance computing enables automated statistical inference of multi-scale models. *Cell Syst.* **4**(2), 194–206 (2017)
14. Kaina, B.: DNA damage-triggered apoptosis: critical role of DNA repair, double-strand breaks, cell proliferation and signaling. *Biochem. Pharmacol.* **66**(8), 1547–1554 (2003)
15. Kim, M., Gillies, R.J., Rejniak, K.A.: Current advances in mathematical modeling of anti-cancer drug penetration into tumor tissues. *Front. Oncol.* **3**, 278 (2013)
16. Louzoun, Y., Xue, C., Lesinski, G.B., Friedman, A.: A mathematical model for pancreatic cancer growth and treatments. *J. Theor. Biol.* **351**, 74–82 (2014)
17. Lazarz, R.: Graph-based framework for 3-D vascular dynamics simulation. *Procedia Comput. Sci.* **101**, 415–423 (2016)
18. Masunaga, S.I., Ono, K., Hori, H., Suzuki, M., Kinashi, Y., Takagaki, M.: Potentially lethal damage repair by total and quiescent tumor cells following various DNA-damaging treatments. *Radiat. Med.* **17**(4), 259–264 (1999)
19. Ribba, B., Holford, N.H., Magni, P.: A review of mixed-effects models of tumor growth and effects of anticancer drug treatment used in population analysis. *CPT Pharmacomet. Syst. Pharmacol.* **3**, e113 (2014)
20. Ribba, B., Holford, N.H., Magni, P., Trocóniz, I., Gueorguieva, I., Girard, P.: A review of mixed-effects models of tumor growth and effects of anticancer drug treatment used in population analysis. *CPT: Pharmacomet. Syst. Pharmacol.* **3**(5), 1–10 (2014)
21. Ribba, B., et al.: A tumor growth inhibition model for low-grade glioma treated with chemotherapy or radiotherapy. *Clin. Cancer Res.* **18**(18), 5071–5080 (2012)
22. Rieger, H., Fredrich, T., Welter, M.: *Eur. Phys. J.* **131**, 31 (2016)
23. Weislo, R., Dzwinel, W., Yuen, D.A., Dudek, A.Z.: A 3-D model of tumor progression based on complex automata driven by particle dynamics. *J. Mol. Model.* **15**(12), 1517 (2009)
24. Wodarz, D., Komarova, N.L.: *Dynamics of Cancer: Mathematical Foundations of Oncology*, p. 532. World Scientific, Singapore (2014)
25. Xie, H., Jiao, Y., Fan, Q., Hai, M., Yang, J., Hu, Z., et al.: Modeling Three-dimensional Invasive Solid Tumor Growth in Heterogeneous Microenvironment under Chemotherapy (2018). arXiv preprint [arXiv:1803.02953](https://arxiv.org/abs/1803.02953)